



Effect of System Pressure on Liquid Film Behavior in Horizontal Annular Flow

Ning Zhao¹, Tian Zhang¹, Xianle Zang^{2,*}, Long Xu^{2,*}, Jing Wang²

¹College of Quality and Technical Supervision, Hebei University, Baoding, China

²Hebei Baisha Tobacco Co.,Ltd. Baoding Cigarette Factory Safety Management Department, Baoding, China
E-mail (corresponding author): zangxianle@yeah.net, byxl123456@163.com

Abstract

The measurement of liquid film parameters is of great significance in the momentum transfer and heat transfer characteristics of gas-liquid two-phase in annular flow. The liquid film at the bottom of the horizontal annular flow is the thickest and produces the greatest influence on the nature of the annular flow. In large diameter horizontal pipes, the effect of pressure on liquid film behavior lacks systematic discussion. Therefore, a dynamic measurement system for annular flow liquid film was designed based on near-infrared(NIR) sensing technology to complete the measurement of annular flow liquid film thickness data under five pressures. The average liquid film thickness at the bottom is obtained by variational modal decomposition(VMD) of the time series signal, and the wave velocity parameter is obtained by mutual correlation velocimetry. The article initially discusses the effect of pressure on the average thickness of the bottom liquid film as well as the interfacial wave velocity.

1. Introduction

Annular flow is one of the typical models of gas-liquid two-phase flow, which is widely used in nuclear power, aerospace, petrochemical and other fields in industry. After the annular flow liquid film at the end of the boiler water-cooled wall tube bundle is evaporated, the heat transfer deterioration area will appear; in the falling film cooler, the characteristics of the liquid film will directly affect the heat transfer efficiency of the medium on both sides of the tube wall. Therefore, the measurement and research of liquid film parameters under different working conditions is an important basis to ensure the performance of the above facilities. The liquid film at the bottom of the horizontal annular flow is the thickest and has the greatest impact on the properties of the annular flow [1], so the focus of the study is on the bottom liquid film parameters.

Presently, the thickness of the liquid film is mostly measured by experiments, mainly by the electrical method [2,3] and the optical method [4,5]. The electrical conductivity method has high precision for the measurement of liquid film thickness, but it ignores the instantaneous information of liquid film fluctuation due to the influence of resolution. With the development of optics and digital image processing technology, optical methods are widely used in the study of gas-liquid two-phase flow. In addition to the requirements for the light environment of the experimental pipe section, the optical method has a relatively simple structure and measurement principle, and has no fluid interference, so it is better in capturing details. Charogiannis *et al* [6] used particle tracking velocimetry and particle image velocimetry to study films, comparing the analytical solution of film thickness measurements solutions with

measured local velocities. However, high-speed camera technology is greatly affected by optics, and the amount of data is large and the information is redundant. In recent years, near-infrared technology has been applied in the detection of two-phase flow. Julien *et al* [7] proposed a method of synchronizing the film thickness map obtained by thermal imaging image and near-infrared light absorption imaging in the film, which reduces the correlation between boundary layer thickness and temperature. Mithran *et al* [8] used an infrared transceiver to analyze the signal characteristics of the device to measure the thickness of the liquid film and the length of the gas bomb. The Near Infrared NIR absorption method belongs to the point liquid film measurement method with high temporal and spatial resolution. According to Lambert Beer's law, the light intensity has a definite functional relationship with the liquid film thickness. Near-infrared sensors can capture instantaneous change information, eliminate optical interference through signal processing, and effectively extract liquid film parameter change information.

In the horizontal direction, the annular flow film is characterized by an asymmetric distribution. Liquid film thickness at the bottom of the pipe is thicker than at the top. The horizontal circulation has been extensively studied for decades. In 1991, Paras *et al* [9] studied the effect of gas-liquid velocity and circumferential angle of the annular flow of 50.8mm inner diameter horizontal pipe on the symmetry of the circumferential distribution of liquid film thickness by experimental method. In 1998, Shedd *et al* [10] applied the principle of optical reflection to carry out static experiments of liquid film thickness and dynamic experiments of circumferential liquid film thickness of gas-liquid two-phase annular flow in horizontal pipes. In 2011, Farias *et al* [11] used laser-



induced fluorescence technology to study the variation law of liquid film thickness for gas-liquid two-phase flow in a horizontal tube with an inner diameter of 15 mm. The results show that the average liquid film thickness at the bottom is a decreasing function of the gas superficial velocity. In 2017, Setyawan *et al* [12] summarized the distribution law of liquid film thickness of gas-liquid two-phase annular flow in a horizontal pipe with an inner diameter of 26 mm, and measured the average liquid film thickness at the bottom under different liquid superficial velocities. Most studies address the effects of gas and liquid superficial velocities, pipe diameters, and other flow characteristics, but lack of discussion of the effect of system pressure on liquid film behavior, especially for larger diameter and horizontal pipes.

Research working on nuclear fuel optimization, evaporator and condenser design, etc. requires obtaining accurate and reliable relationships for liquid film characteristic parameters. This work uses a calibrated near-infrared (NIR) absorption sensor to collect time-series data of liquid film thickness under different pressures. The variational mode decomposition (VMD) method is used to perform time-frequency analysis on the data, and then the thickness of the liquid film is effectively extracted; the interface wave velocity is obtained by the cross-correlation velocimetry technology. In-depth analysis of the liquid film information obtained from the experimental measurements is carried out to study the effect of pressure on the behavior of the liquid film.

2 Measuring system

2.1 Liquid film thickness measurement

NIR absorption follows Lambert Beer law, namely:

$$I(\lambda) = I_0(\lambda) \exp[-k_{abs}(\lambda)L] \quad (1)$$

In the Equation (1), $I_0(\lambda)$ and $I(\lambda)$ are the incident light intensity and transmitted light intensity respectively; k_{abs} is the absorption coefficient at the wavelength λ ; L is the optical path, the unit is m.

A liquid film thickness measurement sensor, a near-infrared absorption (NIR) sensor, is constructed based on Lambert Beer law, as shown in Figure 1. The sensor is mainly composed of two groups of near-infrared absorption detection units. Each group is mainly divided into three parts, namely near-infrared light source, photodetector and optical signal processing module. The laser diode module sends the wavelength of 980 nm to the liquid interface through the light guide tube. After absorption and attenuation by the liquid film, the near-infrared light signal reaches the photodetector, and is modulated, rectified and amplified by the photovoltaic, and the collected output signal stored in the computer. The depth of the light guide tube can be dynamically adjusted, the output wavelength of the transmitting probe is 980 nm (± 10 nm), and the power is 4.5 mW; the

FLOMEKO 2022, Chongqing, China

wavelength range that the detector can receive is 800-1700 nm.

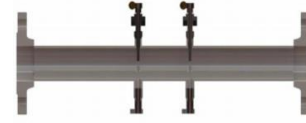


Figure 1: Measurement sensors

2.2 Experimental setup and measurement range

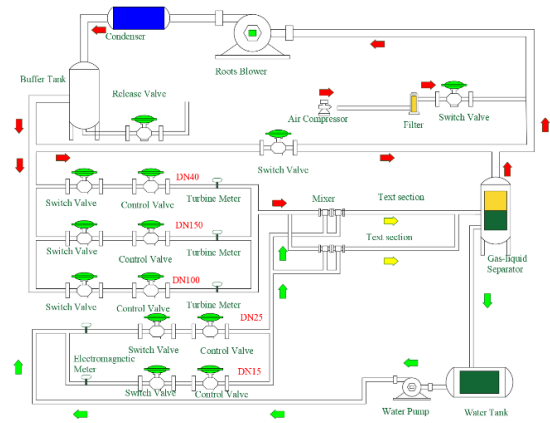


Figure 2: Schematic diagram of experimental facility

Table 1: Experimental condition and range

Pipe pressure (MPa)	Gas superficial velocity (m/s)	Liquid superficial velocity (m/s)	Mass quality x
0.2, 0.4, 0.5, 0.6, 0.8	12.8, 15.6	0.042~0.326	0.121~0.793

The device used in the experiment is shown in Figure 2, which is a double-closed-loop adjustable-pressure medium-pressure wet gas experimental device. The experimental pipeline section is plexiglass with an inner diameter of 50 mm. The device uses a double circulation loop with a working upper limit of 1.6MPa. In the experiment, water and compressed air are used as the flowing medium. In the liquid phase cycle, the water reaches the experimental pipe section after being measured by the booster pump through the electromagnetic flowmeter. In the gas phase cycle, the air is introduced into the Roots blower through the condenser, and then enters the experimental pipe section through the turbine flowmeter and the Roots flowmeter to be mixed with the liquid phase. After the two-phase mixing is fully developed, a stable annular flow is formed, which finally flows into the gas-liquid separation tank, and continues to circulate after separation. Pressure and temperature are collected in real time through pressure transmitters and temperature transmitters. The experimental flow conditions are listed in Table 1.



2.3 Calibration of the measurement system

The measurement accuracy of the characteristic parameters of the gas-liquid two-phase annular flow interface wave depends on the measurement accuracy of the liquid film thickness. Due to the fluctuation of the liquid film surface, the measurement results of the liquid film thickness measurement sensor are inconsistent with the real values, which will inevitably cause interface waves. The accuracy of the characteristic parameters cannot be guaranteed, so it is necessary to calibrate the sensor liquid film thickness measurement.

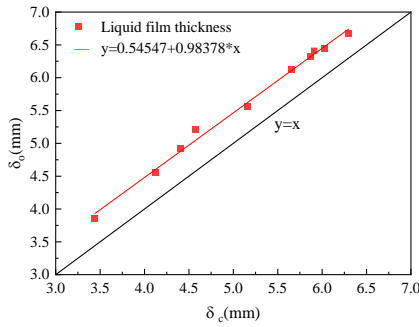


Figure 3: The results of dynamic calibration

(δ_0 -Time-averaged liquid film thickness measured by the NIR sensor, δ_c -Time-averaged liquid film thickness measured by the conductance probe)

Because the Lambert Beer absorption coefficients are obtained under strict experimental conditions using pure or distilled water, and the experimental water contains some impurities or particles more or less. Furthermore, due to the existence of two-phase interface fluctuations, these factors will cause a certain loss of light energy. So, the measured value of the liquid film thickness is too large. Dynamic calibration of NIR liquid film thickness measurement sensors. The calibration results are shown in Figure 3. According to the requirements of measurement accuracy, the absorption coefficient value is corrected by the above calibration results.

3 Data calculation

3.1 Principle of VMD algorithm

VMD is a signal processing method proposed by Dragomiretskiy *et al* [13]. The method iteratively searches for the optimal solution of the variational model, minimizes the sum of the estimated bandwidths of each mode, and realizes the adaptive decomposition of the signal. It solves the shortcomings of modal aliasing in the decomposition process, and the components with similar frequencies cannot be correctly separated.

(1) Build a variational equation

Hilbert transform:

$$\left[\delta(t) + \frac{j}{\pi t} \right] \times u_k(t) \quad (2)$$

For the modal function $u_k(t)$ estimate the central frequency $e^{-j\omega_k t}$ of each mode of the analytical signal,

FLOMEKO 2022, Chongqing, China

and then transfer the transformed modal function spectrum to baseband:

$$\left[\delta(t) + \frac{j}{\pi t} \right] \times u_k(t) e^{-j\omega_k t} \quad (3)$$

(2) The variational problem can be transformed into a problem of seeking K modal functions to solve:

$$\begin{cases} \min_{\{u_k\}, \{\omega_k\}} \left\{ \sum_k \left\| \partial_t \left[\left(\delta(t) + \frac{j}{\pi t} \right) * u_k(t) \right] e^{-j\omega_k t} \right\|_2^2 \right\} \\ \text{s.t.} \sum_{k=1}^K u_k(t) = f(t) \end{cases} \quad (4)$$

(3) Solving the variational equation

In order to obtain the optimal solution of the above variational problem, a penalty factor α and a Lagrange multiplication operator λ are introduced into the variational problem.

$$\begin{aligned} \mathcal{L}(\{u_k\}, \{\omega_k\}, \lambda) = & \alpha \sum_k \left\| \partial_t \left[\left(\delta(t) + \frac{j}{\pi t} \right) * u_k(t) \right] e^{-j\omega_k t} \right\|_2^2 \\ & + \left\| f(t) - \sum_k u_k(t) \right\|_2^2 + \left\langle \lambda(t), f(t) - \sum_k u_k(t) \right\rangle \end{aligned} \quad (5)$$

Update iteratively to $u_k^{n+1}(t)$, ω_k^{n+1} , $\lambda^{n+1}(t)$. The minimum value of the extended Lagrange expression is found. Then, \hat{u}_k is minimized as:

$$\hat{u}_k^{n+1}(\omega) = \frac{f(\omega) - \sum_{i=k}^{\hat{}} \hat{u}_i(\omega) + \frac{\hat{\lambda}(\omega)}{2}}{1 + 2\alpha(\omega - \omega_k)^2} \quad (6)$$

ω_k^{n+1} is minimized to:

$$\omega_k^{n+1} = \frac{\int_0^{+\infty} \omega \left| \hat{u}_k(\omega) \right|^2 d\omega}{\int_0^{+\infty} \left| \hat{u}_k(\omega) \right|^2 d\omega} \quad (7)$$

λ is the Lagrange multiplier, and the updated equation is:

$$\lambda^{n+1} = \lambda^n + \tau \left(x - \sum_{k=1}^K u_k^{n+1} \right) \quad (8)$$

ε is the noise margin that meets the requirements of signal decomposition fidelity. The iteration ends when the equation satisfies Equation (8):

$$\sum_{k=1}^K \frac{\|u_k^{n+1} - u_k^n\|_2^2}{\|u_k^n\|_2^2} < \varepsilon \quad (9)$$

3.2 Cross-correlation wave velocity measurement



The measurement of the interface wave velocity is realized by the cross-correlation technique. The basic principle of the measurement is to convert the interface wave velocity measurement into the time interval measurement of similar signals through the similarity analysis of the time series of the upstream and downstream transmitted light intensity signals based on the liquid film measurement. Perform cross-correlation operation on the upstream light intensity signal $y_1(t)$ and the downstream light intensity signal $y_2(t)$, then the cross-correlation function $R_{12}(\tau)$ is:

$$R_{12}(\tau) = \lim_{T \rightarrow \infty} \frac{1}{T} \int_0^T y_1(\tau) y_2(t - \tau) dt \quad (10)$$

The time τ_0 corresponding to the peak value of the cross-correlation function R_{12} is the transit time τ between the upstream and downstream signals. The fluctuation average velocity u_w on the measurement section can be obtained by Equation (11), where S is the distance between probes.

$$u_w = S / \tau_0 \quad (11)$$

4 Results and Discussion

4.1 Analysis of VMD effect

For the variational modal decomposition of the liquid film thickness time series signal, the key problem in the VMD algorithm is to preset parameters such as penalty factor, modal decomposition series, and convergence conditions. Take the system pressure $P=0.4\text{MPa}$, $=0.099\text{m/s}$, $u_{sg}=15.6\text{m/s}$ as an example to decompose the signal. The decomposition effect is shown in Figure 4. Figure 4 shows the signal distribution on the left and the central frequency on the right. During the process, the liquid film signal is decomposed into 6 layers of IMF1-IMF6, and the central frequencies of each layer do not overlap each other. The mean is [1.58, 34.66, 77.22, 138.25, 226.68, 360.02]. The central frequency of IMF1 representing the real signal of liquid film thickness is around 1.58Hz, the central frequency of IMF2-IMF4 is distributed around 50Hz multiples, which are power frequency interference noise. The central frequency of IMF6 is higher than 300 Hz, which is random noise caused by droplet scattering and refraction, and the power spectrum and energy account for a small proportion. Due to the irregularity of the disturbance wave, the spike interference is caused by the reflection, scattering, refraction and other factors of the light. In the IMF1 decomposed by VMD, the amplitude is significantly reduced, reflecting the characteristics of disturbance waves, as shown by the red box in the Figure 4. At the same time, VMD decomposition decomposes random interference into high frequency parts.

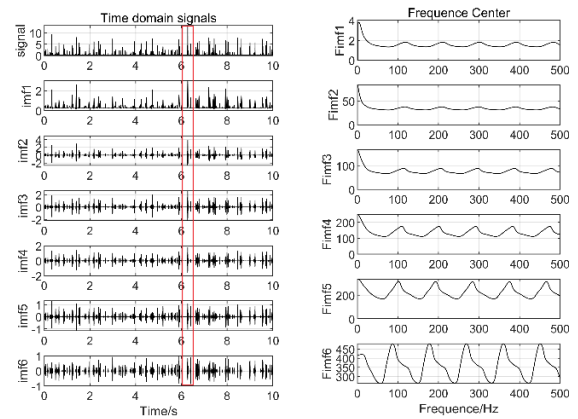


Figure 4: Liquid film thickness signal decomposed by VMD

4.2 Average liquid film thickness at the bottom

The liquid film at the bottom of the annular flow of the horizontal tube is the thickest, which has a great influence on the properties of the annular flow. The average thickness of the bottom liquid film is mainly discussed in this section. Figure 5 shows the time domain fluctuation diagram of the liquid film thickness of different liquid superficial velocity (0.099m/s, 0.170m/s, 0.227m/s) under $P=0.2\text{MPa}$, $u_{sg}=15.6\text{m/s}$. With the increase of liquid flow velocity, the average thickness of the liquid film at the bottom increases gradually.

As shown in Figure 6, the thickness of the bottom liquid film increases with the increase of the superficial velocity of the liquid phase, and correspondingly decreases with the increase of the apparent flow velocity of the gas phase. The trend is consistent with previous studies [5], and it can better illustrate the effect of system pressure on the thickness of the liquid film at the bottom in the pipeline. The variation of the liquid film thickness with the system pressure under different liquid flow velocity is shown in Figure 6. Under the condition of constant u_{sg} , the liquid film thickness gradually becomes thicker with the increase of liquid flow velocity. Under the condition of constant u_{sl} and u_{sg} , the liquid film thickness becomes thinner obviously with the increase of pressure. Under the condition of pressure, the shearing effect of the gas-liquid interface shear force on the disturbance wave becomes larger, resulting in entrained droplets, which enter the gas core and reduce the thickness of the liquid film on the tube wall. The same rule applies to other gas-liquid flow points.

4.3 Wave velocity

Under the condition of the horizontal pipe, the interface wave exhibits obvious fluctuation characteristics due to the high gas velocity of the gas-liquid two-phase annular flow. Wave velocity is one of the most important parameters to describe the characteristics of disturbance waves. The analysis and study of the influence of pressure on the surface disturbance wave velocity at the bottom of the horizontal pipe is mainly aimed at in this section.

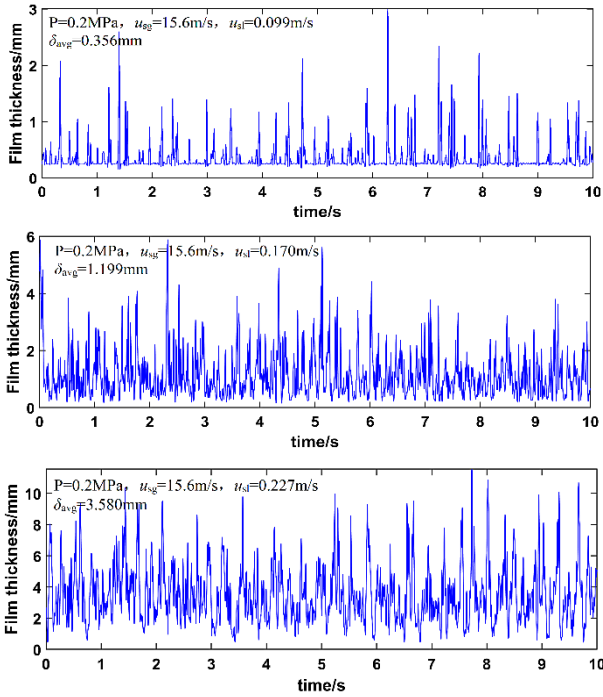


Figure 5: Fluctuation graph of liquid film thickness for three working conditions

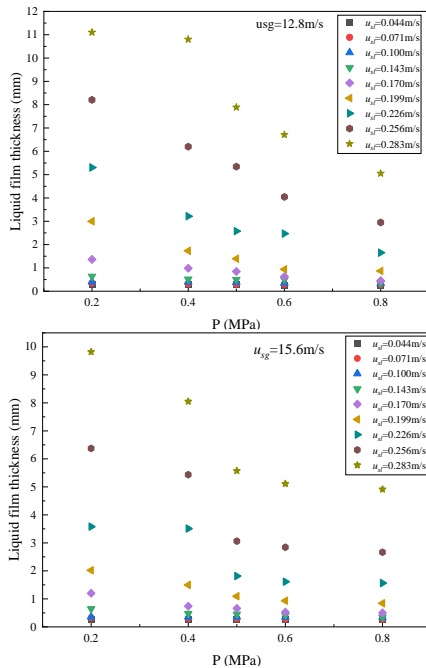


Figure 6: Effect of pressure on average liquid film thickness.

When the system pressure $P=0.2\text{MPa}$, the change of the wave velocity parameters with the gas-liquid two-phase flow velocity is shown in Figure 7. When u_{sl} is constant, the wave velocity of the disturbance increases significantly with the increase of the gas superficial velocity. In addition, when u_{sg} is constant, the wave velocity increases with the increase of liquid superficial velocity, which is almost a linear growth. When the FLOMEKO 2022, Chongqing, China

superficial velocity of the liquid phase increases, the thickness of the liquid film becomes thicker. The retardation of the liquid phase by the wall surface becomes smaller, the interphase shear force increases, and the wave speed increases accordingly. When the gas superficial velocity increases, the liquid film is sheared by the high-velocity gas. The greater the gas velocity, the stronger the shearing effect, the more momentum the liquid film obtains, and the larger the wave speed. The same rules apply at other pressure points.

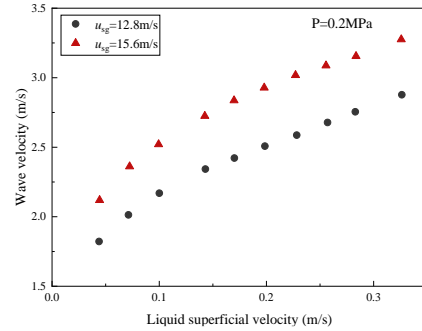


Figure 7: Effect of gas and liquid superficial velocity on wave velocity.

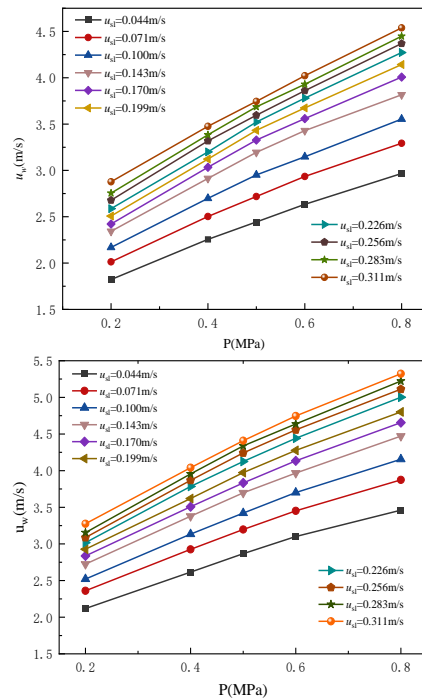


Figure 8: Effect of pressure on wave velocity

The relationship between the wave velocity and the pressure is shown in Figure 8. The wave velocity increases with the pressure and the superficial velocity of the gas and liquid phases. It can be seen from the results that the increase of pressure has a significant effect on the increase of the wave velocity of the liquid film. At a constant gas superficial velocity, the wave velocity increases almost linearly with pressure. The increase in pressure causes the gas density to increase exponentially, transferring more momentum from the gas core to the



liquid film. The shear force at the gas-liquid interface increases with the increase of pressure, and the shear force reduces the fluctuation amplitude of the disturbance wave. As a result, more and more disturbance waves with smaller and more regular amplitudes are formed, so the wave velocity is getting faster and faster.

5 Conclusion

Based on the near-infrared sensor, the dynamic measurement system of the liquid film of the horizontal annular flow was designed, and the bottom liquid film information data was collected under the system pressure of 0.2MPa to 0.8Mpa. Based on the experiment, the wave velocity and thickness of the liquid film at the bottom are quantitatively analysed, and the trends are studied. The conclusions are as follows:

(1) The average thickness of the bottom liquid film increases with the liquid superficial velocity and decreases with the gas flow velocity. The effect of pressure on the thickness of the liquid film changes significantly. With the increase of the pressure, the shear force at the interface increases, and the interfacial disturbance wave peak is sheared to produce entrained droplets. The droplets entering the gas core will reduce the thickness of the liquid film.

(2) The wave velocity of the liquid film at the bottom increases with the increase of the superficial velocity of gas and liquid. Moreover, there is a direct relationship between wave velocity and pressure. Under pressure conditions, the density of the gas phase becomes larger and larger. More momentum is transferred from the gas core to the liquid film, and the shear force at the gas-liquid interface is increasing. There are more and more regular disturbance waves, so the wave speed increases.

Acknowledgements

This study is supported by the Natural Science Foundation of Hebei Province, China (F2021201031)、(F2022201034)

References

- [1] Shedd T A, Newell T A, “Characteristics of the liquid film and pressure drop in horizontal, annular, two-phase flow through round, square and triangular tubes”, *Journal of Fluids Engineering*, **Vol.126**(5), pp.807-817, 2004.
- [2] Zhao Y, Markides C N, Matar O K, Hewitt G F, “Disturbance wave development in two-phase gas-liquid upwards vertical annular flow”, *International Journal of Multiphase Flow*, **Vol.55**, pp.111-129, 2013.
- [3] Abdulkadir M, Mbalisigwe U P, Zhao D, Hernandez-Perez V, Azzopardi B J, Tahir S, “Characteristics of churn and annular flows in a large diameter vertical riser”, *International Journal of Multiphase Flow*, **Vol.113**, pp.250-263, 2019.
- [4] Alekseenko S V, Cherdantsev A V, Heinz O M, Kharlamov S M, Markovich D M, “Analysis of spatial and temporal evolution of disturbance waves and ripples in annular gas-liquid flow”, *International Journal of Multiphase Flow*, **Vol. 67**, pp.122–134,2014.
- [5] Dasgupta A, et al., “Experimental investigation on dominant waves in upward air-water two-phase flow in churn and annular regime”, *Experimental Thermal and Fluid Science*, **Vol. 81**, pp.147–163,2017.
- [6] Charogiannis A, Sik J, Voulgaropoulos V, Markides C.N, “Structured planar laser-induced fluorescence (S-PLIF) for the accurate identification of interfaces in multiphase flows”, *International Journal of Multiphase Flow*, **Vol.118**, pp. 193–204,2019.
- [7] Julien D, Guillaume M, Domenico P, et al, “Mid wave infrared thermography of water films in condensing and evaporating environments”, *Nuclear Engineering and Design*, **Vol.336**, pp80–89,2018.
- [8] Mithran N, Venkatesan M, “Signal characteristics of IR transceiver pair during two phase flow of varying liquid film thickness in a mini-channel”, *Chemical Engineering Communications*, **Vol.208**(6), pp.870–882, 2021.
- [9] Paras S M, Karabelas A J, “Properties of the liquid layer in horizontal annular flow”. *International Journal of Multiphase Flow*, **Vol.17**(4), pp.439–454,1991.
- [10] Shedd T A, and. Newell T A, “Automated optical liquid film thickness measurement method”, *Review of Scientific Instruments*, **Vol.69**(12), pp.4205–4213,1998.
- [11] Farias P S C, Martins F J W A, Sampaio L E B, et a l, “Liquid film characterization in horizontal, annular , two-phase, gas-liquid flow using time-resolved laser-induced fluorescence”, *Experiments in Fluids*, **Vol.52**(3), pp.633-645,2012.
- [12] Setyawan A, Indarto, Deendarlianto.“Experimental investigations circumferential liquid film distribution of air-water annular two-phase horizontal pipe”, *Experimental Thermal and Fluid Science*, **Vol.85**, pp.95-118, 2017.
- [13] Dragomiretskiy K, Zosso D, “Variational mode decom-position”, *IEEE Transactions on Signal Processing*, **Vol .62**(3), pp.531-544,2014.